Journal of Materials Chemistry A

Accepted Manuscript

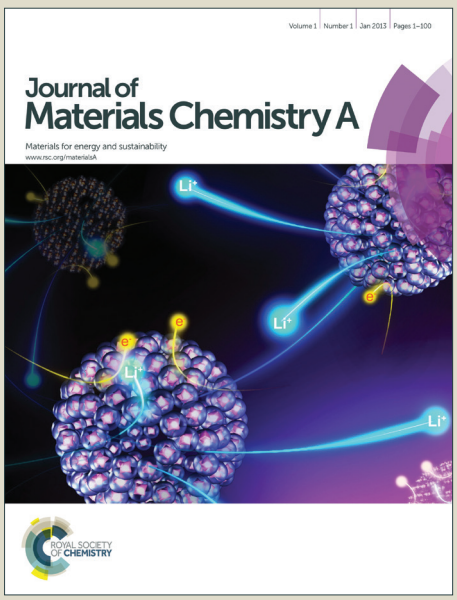

This is an *Accepted Manuscript*, which has been through the Royal Society of Chemistry peer review process and has been accepted for publication.

Accepted Manuscripts are published online shortly after acceptance, before technical editing, formatting and proof reading. Using this free service, authors can make their results available to the community, in citable form, before we publish the edited article. We will replace this *Accepted Manuscript* with the edited and formatted *Advance Article* as soon as it is available.

You can find more information about *Accepted Manuscripts* in the Information for Authors.

Please note that technical editing may introduce minor changes to the text and/or graphics, which may alter content. The journal's standard Terms & Conditions and the Ethical guidelines still apply. In no event shall the Royal Society of Chemistry be held responsible for any errors or omissions in this *Accepted Manuscript* or any consequences arising from the use of any information it contains.

ROYAL SOCIETY OF CHEMISTRY

www.rsc.org/materialsA

Journal Name

RSCPublishing

ARTICLE

Ethanol-assisted hydrothermal synthesis of $LiNi_{0.5}Mn_{1.5}O_4$ with excellent long-term cyclability at high rate for lithium-ion batteries

Cite this: DOI: 10.1039/x0xx00000x

Yuan Xue[a], Zhenbo Wang[a]*, Fuda Yu[a], Yin Zhang[a] and Geping Yin[a]

Received 00th January 2013,
Accepted 00th January 2013

DOI: 10.1039/x0xx00000x

www.rsc.org/

High voltage spinel $LiNi_{0.5}Mn_{1.5}O_4$ has been synthesized by an ethanol-assisted hydrothermal method. The $LiNi_{0.5}Mn_{1.5}O_4$ has also been synthesized by precipitation method and hydrothermal method for comparison. The materials were characterized by X-ray diffraction, raman spectroscopy, scanning electron microscope, X-ray photoelectron spectroscopy and electrochemical tests. The ethanol-assisted hydrothermal process improves the dispersity and decreases the size of particles in the presence of ethanol. With small size particle, the $LiNi_{0.5}Mn_{1.5}O_4$ had excellent rate capability. Its discharge capacity is 81.7 mAh g^{-1} at a high rate of 20 C. On the other hand, the ethanol-assisted hydrothermal process mixs the reagents homogeneously and improves the crystallinity. It leads to low impurity and Mn^{3+} ions contents, which are beneficial to electrochemical performance. The $LiNi_{0.5}Mn_{1.5}O_4$ exhibits remarkable long-term cyclability. After 1000 cycles at 5 C discharge rate, its discharge capacity is 102.1 mAh g^{-1} with capacity retention ratio of 88.1%. It also has good high temperature performance with capacity retention of 82.0% after 200 cycles at 55 ^oC.

Introduction

High energy and high power rechargeable lithium-ion batteries have become dominant power sources for electric drive vehicles and hybrid electric vehicles available in the market. One strategy of increasing the power density and capacity of lithium ion batteries is to raise its operation voltage by utilizing high-voltage positive electrode. Among cathode materials, $LiNi_{0.5}Mn_{1.5}O_4$ has received great attention for its good electrochemical properties with a potential plateau at around 4.7 V and its low cost.[1-7] The $LiNi_{0.5}Mn_{1.5}O_4$ has cubic spinel structure where Li and O occupy the 8a tetrahedral sites and 32e sites, respectively, while Ni and Mn cations occupy the octahedral sites.[8] This can provide a three dimensional pathway for lithium ion diffusion.

As a cathode material, long-term cycling stability is requisite for $LiNi_{0.5}Mn_{1.5}O_4$ to meet application demands of LIBs for portable electronics, EVs and HEVs. On the other hand, $LiNi_{0.5}Mn_{1.5}O_4$ is a promising cathode to couple with the $Li_4Ti_5O_{12}$ anode and fabricate the 3V lithium-ion battery. While the $Li_4Ti_5O_{12}$ has good long-term cyclability due to its zero-strain in the charge-discharge process.[9,10] So the $LiNi_{0.5}Mn_{1.5}O_4$ should have equivalent long-term cyclability. Fang et al. have improved its long-term cyclability by graphene oxide coating and the $LiNi_{0.5}Mn_{1.5}O_4$ showed 61% capacity retention after 1000 cycles at 0.5C.[11]

$LiNi_{0.5}Mn_{1.5}O_4$ has been synthesized by solid-state method,[12,13] co-precipitation method[14,15] and solution evaporation method.[16] Sun et al. synthesized $LiNi_{0.5}Mn_{1.5}O_4$ by precipitation method with hydrothermal treatment.[17] They find that hydrothermal process improvs crystallinity and particle sizes. However, the obtained $LiNi_{0.5}Mn_{1.5}O_4$ contained Mn^{3+} ions and $Li_xNi_{1-x}O$ impurity. The appearance of secondary phases and Mn^{3+} is caused by loss of oxygen at high temperature calcination.[18,19] The high impurity and Mn^{3+} contents have adverse effects on electrochemical properties. However, the oxygen loss occurring at high temperatures can be recovered by annealing of low rate cooling, which can also reduce impurity and Mn^{3+} amount.[20,21]

In this paper, we report an ethanol-assisted hydrothermal method to synthesize $LiNi_{0.5}Mn_{1.5}O_4$. Ethanol was added to control particle growth. With the same annealing of low rate cooling, we compared the impurity and Mn^{3+} contents of ethanol-assisted hydrothermal method, hydrothermal method and precipitation method and discussed the influence of Mn^{3+} on cycle performance. The $LiNi_{0.5}Mn_{1.5}O_4$ obtained by ethanol-assisted hydrothermal method showed excellent long-term cyclability at high discharge rate.

Journal of Materials Chemistry A Accepted Manuscript

Experimental

Preparation of $LiNi_{0.5}Mn_{1.5}O_4$

$LiNi_{0.5}Mn_{1.5}O_4$ was synthesized by ethanol-assisted hydrothermal method. 8.4 mmol $Li(CH_3COO)\cdot 2H_2O$, 4 mmol $Ni(CH_3COO)_2\cdot 4H_2O$ and 12 mmol $Mn(CH_3COO)_2\cdot 4H_2O$ were dissolved in 50 mL distilled water. Then 10 mL ethanol was added to the solution. After its complete dispersion, the NH_4HCO_3 aqueous solution (2 mol L^{-1}, 50ml) was added to the solution in sequence under stirring. Then the solution was transferred to a 200 ml Teflon-lined stainless steel autoclave. The autoclave was sealed, kept at 180 ^oC for 5 h, and then cooled down naturally to room temperature. The suspension was dried and ground to obtain the precursor. Then the precursor was heated at 400 ^oC for 4 h and 800 ^oC for 10 h in air. Then the mixture was cooled at a rate of 0.5 ^oC min^{-1} in oxygen atmosphere to obtain the product. The $LiNi_{0.5}Mn_{1.5}O_4$ was also synthesized by precipitation method, in which the ethanol-assisted hydrothermal procedure were replaced by stirring at room temperature for 5 h and the other procedures are invariant. And the $LiNi_{0.5}Mn_{1.5}O_4$ was also synthesized by hydrothermal method, in which no ethanol was added and the other procedures are the same with ethanol-assisted hydrothermal method.

Charaterization of $LiNi_{0.5}Mn_{1.5}O_4$

The obtained material was characterized by scanning electron microscope (SEM) using a Quanta-200 and powder X-ray diffraction (XRD). XRD was performed with a D/max-RB diffractometer using Cu Kα source and recorded with a step of 0.05°. And the raman spectra were obtained with a Renishaw in Via Raman microscope. X-ray photoelectron spectroscopy (XPS) was carried out by using the Physical Electronics PHI model 5700 instrument.

The electrochemical tests were carried out in Coin-type cells (CR 2025). The cells were assembled in an argon-filled glove box. A slurry containing 80 wt.% active material, 10 wt.% conductive acetylene black and 10 wt.% polyvinylidene fluoride was cast onto an aluminum foil using a blade and dried at 120 ^oC in a vacuum oven for 12h. Then the foil was punched into circular electrode 1.4 cm in diameter. Its loading weight was about 2 mg cm^{-2}. Lithium metal was used as the counter electrode. The electrolyte was 1 mol L^{-1} $LiPF_6$ in a mixture of ethylene carbonate and dimethyl carbonate. The charge-discharge tests were performed on a NEWWARE battery tester. When current densities were higher than 0.5 C, the cells were first charged galvanostatically to 4.95 V at 1 C, and then the voltage was kept at 4.95 V until the current decreased to 0.1 C. Then the cells were discharged to 3.5 V at different rates. Cyclic voltammetry (CV; 3.5-5.1 V, 0.1 mV s^{-1}) and electrochemical impendence spectroscope (EIS) measurements were performed on a CHI650D electrochemical workstation. EIS measurements were conducted with an AC amplitude of 5 mV at 4.73 V in the frequency range from 10^5 Hz to 0.01 Hz.

Results and discussion

Firstly, the $LiNi_{0.5}Mn_{1.5}O_4$ was synthesized by ethanol-assisted hydrothermal method and precipitation method. After adding NH_4HCO_3 into the solution, white precipitation of $MnCO_3$ was observed, while the solution was still green in color, indicating the existence of a large amount of Ni^{2+} ions in solution, owing to strong chelating of Ni^{2+} and NH_3. However, after hydrothermal reaction, the solution became colorless, indicating that Ni^{2+} ions were precipitated during hydrothermal process. Thus the $MnCO_3$ precipitation may serve as crystal nucleus for the precipitation during hydrothermal process.

The XRD patterns of precursors of ethanol-assisted hydrothermal method and precipitation method are showed in Fig. 1. The peaks of precursor of ethanol-assisted hydrothermal method are indexed to the rhombohedral structure of $MnCO_3$ (JCPDS Card No.: 83-1763). The diffraction peaks of precursor of precipitation method are weak, meaning lower crystallinity.

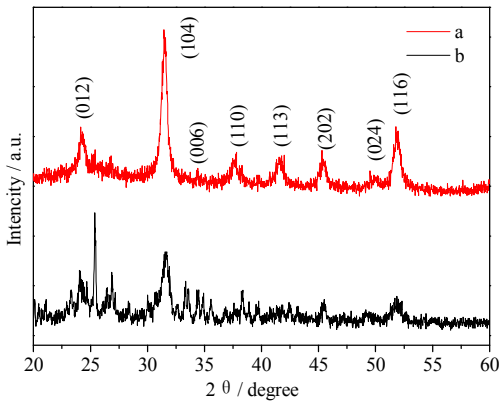

Fig. 1. XRD patterns of precursors prepared by (a) ethanol-assisted hydrothermal method and (b) precipitation method.

Fig. 2 shows the XRD patterns of $LiNi_{0.5}Mn_{1.5}O_4$ synthesized by ethanol-assisted hydrothermal method and precipitation method. Both patterns can be assigned to cubic spinel $LiNi_{0.5}Mn_{1.5}O_4$ (JCPDS Card No.: 80-2162). As shown, the diffraction peaks of $LiNi_{0.5}Mn_{1.5}O_4$ obtained by ethanol-assisted hydrothermal method are stronger and sharper, suggesting its higher crystallinity. The higher crystallinity benefits to high discharge capacity and good cyclability.[22,23] Also, there are some minor residues peaks at 2θ = 37.5, 43.6, and 63.4° that can be attributed to $Li_xNi_{1-x}O$. The peaks of impurity of ethanol-assisted hydrothermal method are much weaker than that of precipitation method, meaning the sample contains very little impurity. During hydrothermal process, $MnCO_3$ crystal grew, meanwhile, Ni^{2+} ions were precipitated. And ethanol improved the dispersivity of the reagents. So the reagents were distributed homogeneously after hydrothermal process and generated $LiNi_{0.5}Mn_{1.5}O_4$ well with low impurity content during calcination at high temperature. The low impurity content is beneficial to the electrochemical properties, due to that the impurity can block Li^+ mobility in material and lead to poor performances.[20]

Journal of Materials Chemistry A Accepted Manuscript

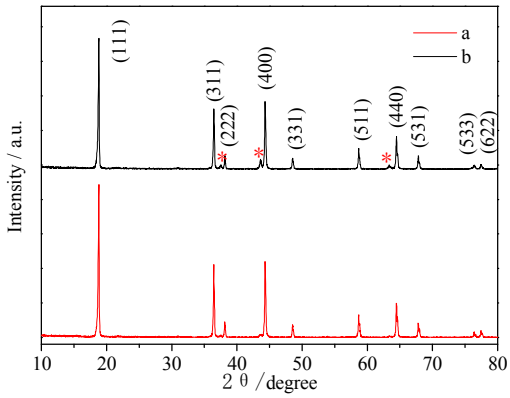

Fig. 2. XRD patterns of $LiN_{i0.5}Mn_{1.5}O_4$ synthesized by (a) ethanol-assisted hydrothermal method and (b) precipitation method.

The nominal spinel $LiNi_{0.5}Mn_{1.5}O_4$ has two different space groups: Fd-3m with disordered Ni and Mn on the octahedral sites, and $P4_332$ with the ordered Ni and Mn. And the $LiNi_{0.5}Mn_{1.5}O_4$ with disordered Fd-3m has higher Li^+ ions diffusion coefficient and electronic conductivity afforded by charge transfer between Ni and Mn .[24-,5] Raman spectroscopy is a useful tool to determine the cation ordering. Fig. 3 shows Raman spectra of $LiNi_{0.5}Mn_{1.5}O_4$ synthesized by different methods. The peaks around 635 cm^{-1} are assigned to the symmetric Mn-O stretching vibration of MnO_6 group and the peaks around 400 and 490 cm^{-1} can be assigned to the Ni^{2+}-O stretching mode. The Raman spectra of both $LiNi_{0.5}Mn_{1.5}O_4$ are indexed to Fd-3m space group, due to the absence of a splitting of peaks in the 588-623 cm^{-1} region, which are characteristic of the ordered structure ($P4_332$) of the spinel.[26,27]

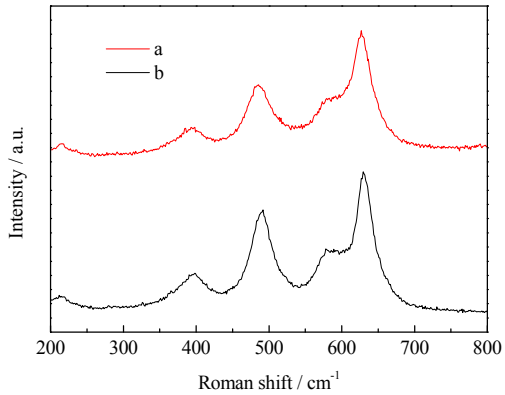

Fig. 3. Raman spectra of $LiNi_{0.5}Mn_{1.5}O_4$ synthesized by (a) ethanol-assisted hydrothermal method and (b) precipitation method.

The hydrothermal process results in large particles sizes.[17] The large particles have smaller specific surface area and longer Li^+ ions diffusion distance, bad for rate capability. Here，ethanol was added to control particle growth. To prove the role of ethanol, the $LiNi_{0.5}Mn_{1.5}O_4$ was synthesized by hydrothermal method without ethanol for comparison. Its XRD pattern in Fig. S1 can be assigned to spinel $LiNi_{0.5}Mn_{1.5}O_4$ and it has very little impurity. The morphology of $LiNi_{0.5}Mn_{1.5}O_4$ synthesized by different methods is presented in the SEM images of Fig. 4 (magnified 10000 times) and Fig. S2 (magnified 5000 and 20000 times).

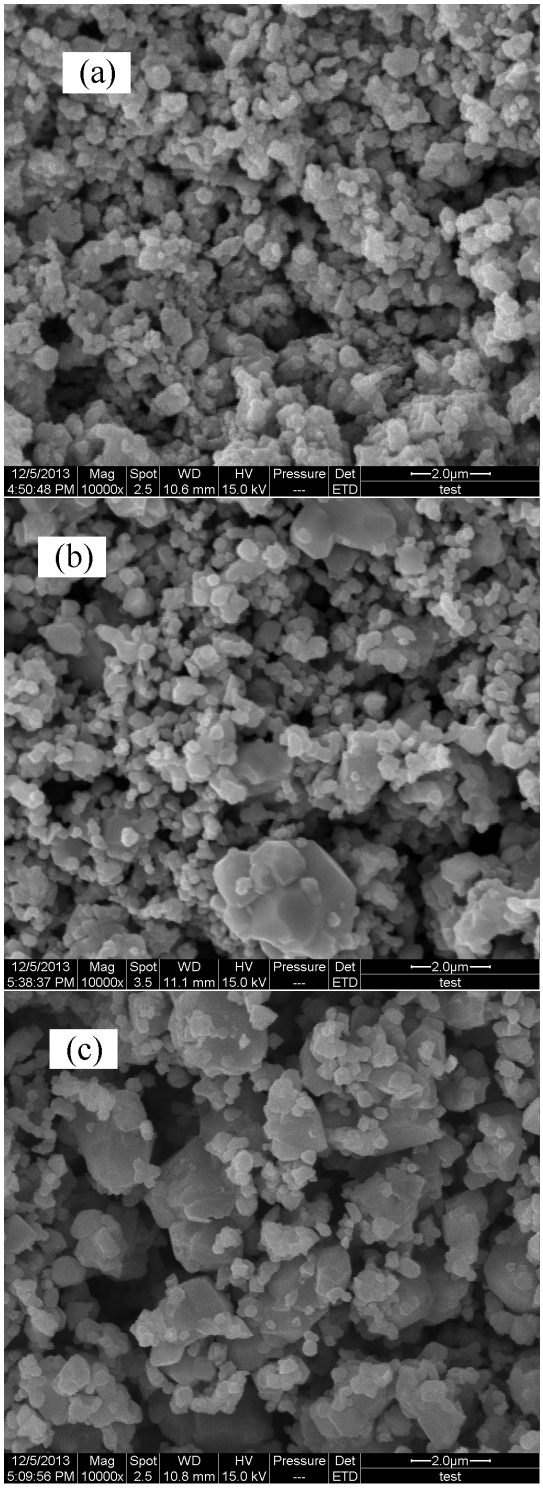

Fig. 4. SEM micrographs of $LiNi_{0.5}Mn_{1.5}O_4$ synthesized by (a) ethanol-assisted hydrothermal method, (b) precipitation method and (c) hydrothermal method.

Journal of Materials Chemistry A Accepted Manuscript

It can be seen that the particle size of sample prepared from hydrothermal method without ethanol is larger than that of precipitation method, meaning that particles grow in the hydrothermal process. However, the particle size of sample prepared from ethanol-assisted hydrothermal method is smallest and there are no large particles about 2 um, compared with those of other methods. The ethanol-assisted hydrothermal process can decrease the size and aggregation degree of particles. When the ethanol with low dielectric constant is added, the dielectric constant of the reaction system was decreased.[28,29] The relationship between the particle radius (r) and the solvent dielectric constant (ε) was described as $1/r = A + B/\varepsilon$, A and B regarded as constants.[28-29] Thus, the decreasing the dielectric constant leads to small particle sizes.

The specific capacities at different discharge rates are showed in Fig. 5. The sample of ethanol-assisted hydrothermal method delivers a high capacity of 141.8 mAh g^{-1} at a rate of 0.2 C. The high capacity of hydrothermal method may be attributed to its higher crystallinity and lower impurity content. Meanwhile, it exhibits better rate performance. At the rates of 5, 15, and 20 C, the corresponding discharge capacities are 108.9, 89.5 and 81.7 mAh g^{-1}. The better rate capability is due to its smaller particle, implying shorter Li^+ ions diffusion distance and larger specific active area for electrochemical reactions. With the largest particle sizes, the sample prepared from hydrothermal method shows poor rate performance. And it shows a poor stability in the test. When the current rate was decreased to 0.2 C, its discharge capacity is lower than its original value, while the sample prepared from precipitation method and ethanol-assisted hydrothermal method can recover.

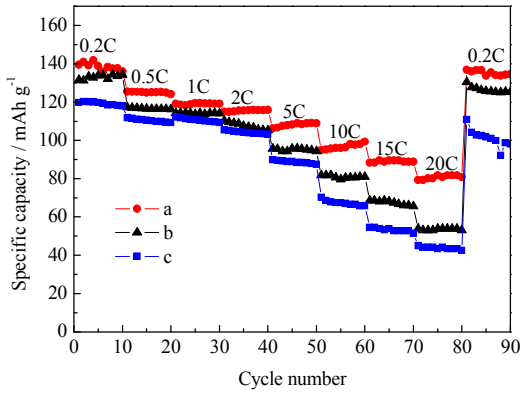

Fig. 5. Rate capacity of $LiNi_{0.5}Mn_{1.5}O_4$ synthesized by (a) ethanol-assisted hydrothermal method (b) precipitation method and (c) hydrothermal method.

Fig. 6 displays the charge and discharge curves of $LiNi_{0.5}Mn_{1.5}O_4$ synthesized by different methods. The curves at low discharge rates have a dominant plateau at around 4.7V, which is attributed to Ni^{2+}/Ni^{4+} redox couple. A minor plateau in 4 V region is also observed associated with the Mn^{3+}/Mn^{4+} redox couple. As shown, the 4 V plateau of sample by ethanol-assisted hydrothermal method is shorter, suggesting lower Mn^{3+} content. The high temperature calcination and annealing processes were the same in these two methods. So the lower Mn^{3+} content was due to the ethanol-assisted hydrothermal process, the only difference between these two methods. The precursor and product of ethanol-assisted hydrothermal method had higher crystallinity than those of precipitation method, proved by XRD. Thus, during calcination process the oxygen is more difficult to lose due to high crystallinity in ethanol-assisted hydrothermal method. And the less oxygen deficiency leads to less Mn^{3+} ions in $LiNi_{0.5}Mn_{1.5}O_4$. In addition, the sample prepared from hydrothermal method also has low Mn^{3+} content, seen from its short 4 V plateau.

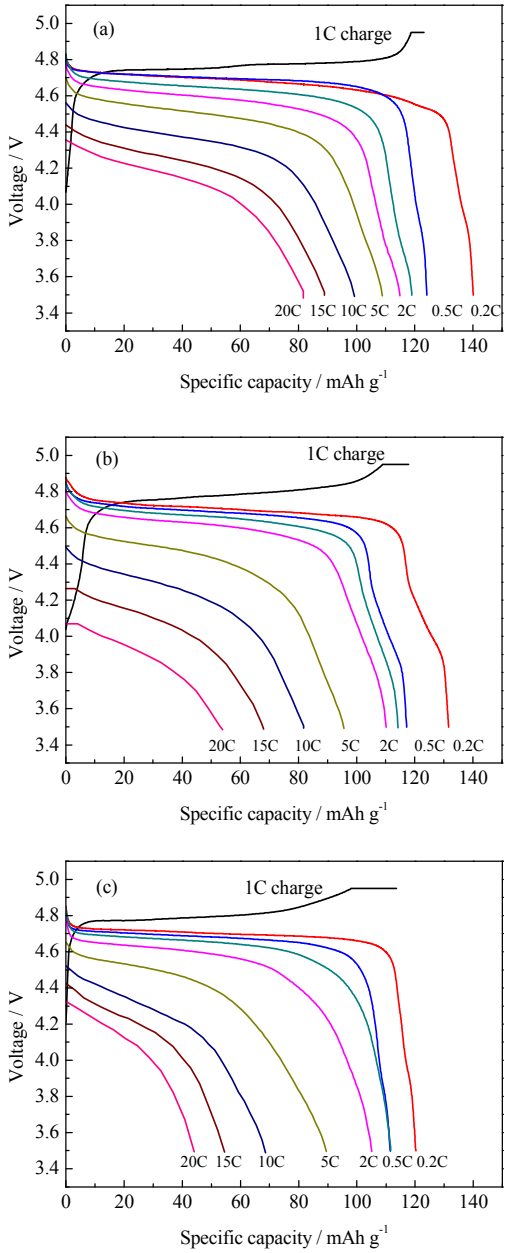

Fig. 6. Charge and discharge capacity curves of $LiNi_{0.5}Mn_{1.5}O_4$ synthesized by (a) ethanol-assisted hydrothermal method, (b) precipitation method and (c) hydrothermal method.

Journal of Materials Chemistry A Accepted Manuscript

Fig. 7 compares the cycling performances for $LiNi_{i0.5}Mn_{1.5}O_4$ synthesized by ethanol-assisted hydrothermal method and precipitation method at rates of 1 C, 2 C and 5 C. For the samples of ethanol-assisted hydrothermal method, the discharge capacities are 130.5, 123.6 and 112.1 mAh g^{-1} after 200 cycles at 1C, 2 C, and 5 C, higher than that by precipitation method. And the sample of ethanol-assisted hydrothermal method has better capacity retention of 96.7 % after 200 cycles at 5 C, than 90.0 % of that by precipitation method. Furthermore, the long cycle performance at 5 C discharge rate of $LiNi_{0.5}Mn_{1.5}O_4$ synthesized by ethanol-assisted hydrothermal method was studied and the capacity and efficiency during cycling are showed in Fig. 8. After 1000 cycles, the discharge capacity of the sample only decreased from 115.9 to 102.1 mAh g^{-1}, corresponding to a high capacity retention of 88.1 %, meaning only 0.012 % capacity decay per cycle. The initial coulombic efficiency is 74.7 %, and it rapidly increased and kept about 97%. It is assumed that the low coulombic efficiency results from the formation of solid electrolyte interphase and the electrolyte decomposition at high voltage.

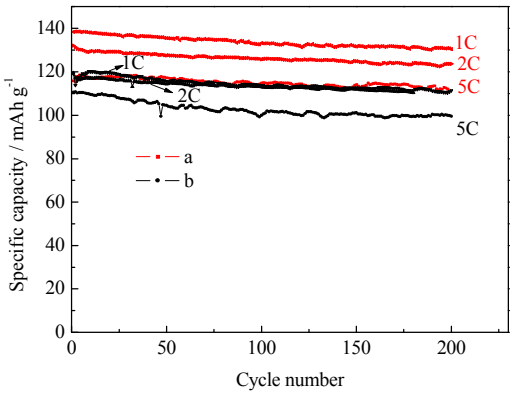

Fig. 7. Cycling performance of $LiNi_{0.5}Mn_{1.5}O_4$ synthesized by (a) ethanol-assisted hydrothermal method and (b) precipitation method at rates of 1 C, 2 C and 5 C.

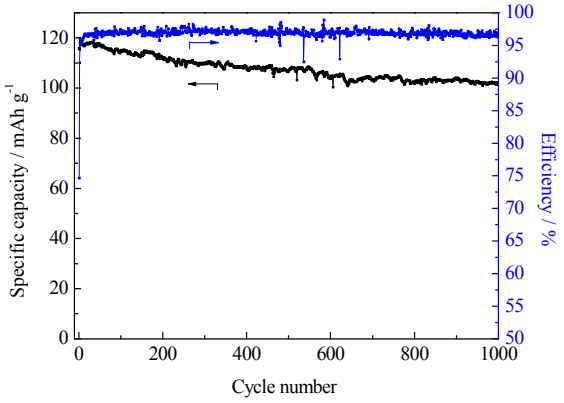

Fig .8. Capacity and efficiency of $LiNi_{0.5}Mn_{1.5}O_4$ synthesized by ethanol-assisted hydrothermal method during cycle at discharge rate of 5 C.

Fig. 9 shows cyclic voltammetry curves of $LiNi_{0.5}Mn_{1.5}O_4$ synthesized by ethanol-assisted hydrothermal method and precipitation method. In both samples, main peaks at around 4.7 V ascribed to the Ni^{2+}/Ni^{4+} redox couples are observed. As shown, the 4.7 V peaks area of the sample by ethanol-assisted hydrothermal method was larger, indicating the sample had a larger specific electrochemically active surface area, consistent with the analysis of morphology above. And after 200 cycles at 5 C rate, the gap between the oxidation and reduction peaks becomes larger, which suggests that the electrochemical reversibility of the cells decreases. Besides, the small peaks at around 4.0 V attributed to the Mn^{3+}/Mn^{4+} redox couple are also observed and magnified in Fig. 9(b). As shown, the peaks area at 4.0 V of the sample of ethanol-assisted hydrothermal method was smaller, meaning the lower Mn^{3+} content, consistent with the analysis of charge and discharge curves. The higher Mn^{3+} content in sample of precipitation method was harmful for the cycle performance, due to the strain from Jahn–Teller distortion of Mn^{3+} and the dissolution of Mn^{2+} into the electrolyte resulted from the disproportionation reaction of Mn^{3+}.

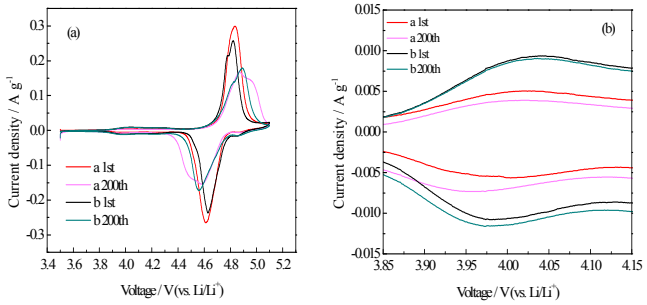

Fig. 9. Cyclic voltammetry curves of $LiNi_{0.5}Mn_{1.5}O_4$ synthesized by (a) ethanol-assisted hydrothermal method and (b) precipitation method before and after 200 cycles at 5 C rate.

In addition, Fig. 10 shows the XPS spectra in the binding energy ranges of Mn $2p_{3/2}$ for $LiNi_{0.5}Mn_{1.5}O_4$ synthesized by ethanol-assisted hydrothermal method and precipitation method before and after 400 cycles at 5C rate. As shown, the Mn $2p_{3/2}$ peak of $LiNi_{0.5}Mn_{1.5}O_4$ synthesized by ethanol-assisted hydrothermal method is located at higher binding energy. Considering that Mn^{4+} and Mn^{3+} each give rise to the Mn $2p_{3/2}$ binding energies at 642.9 and 641.9 eV, the atomic concentrations was estimated by Guassian-Lorentz curve fitting. The relative concentrations of Mn^{3+} of the sample synthesized by ethanol-assisted hydrothermal method before and after cycles are 1.01 % and 4.36 %, lower than 8.95 % and 6.24 % of precipitation method. The results indicate that the $LiNi_{0.5}Mn_{1.5}O_4$ synthesized by precipitation method has a relative higher Mn^{3+} concentration in its surface. And the surface Mn^{3+} ions tend to undergo a disproportionation reaction, $2Mn^{3+} = Mn^{2+} + Mn^{4+}$. The dissolved Mn^{2+} tends to migrate to the anode and finally deposits on the surface of anode. After 400 cycles at 5 C rate, the cells were disassembled and photos of the anodes are showed in Fig. 11. It can be seen that there were more depositions on Li anode in Fig.11 (b), meaning that more Mn

Journal of Materials Chemistry A Accepted Manuscript

ions of $LiNi_{0.5}Mn_{1.5}O_4$ synthesized by precipitation method dissolved into electrolyte and deposited on the anode. The Mn ions dissolution is infaust to the stability of $LiNi_{0.5}Mn_{1.5}O_4$ and the deposition on the surface of anode increases the polarization.

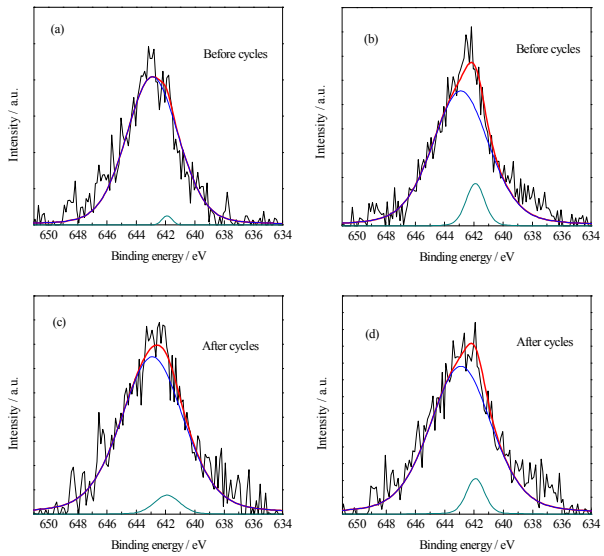

Fig. 10. Mn 2p3/2 XPS spectra of $LiNi_{0.5}Mn_{1.5}O_4$ synthesized by (a,c) ethanol-assisted hydrothermal method and (b,d) precipitation method before and after 400 cycles at 5C rate.

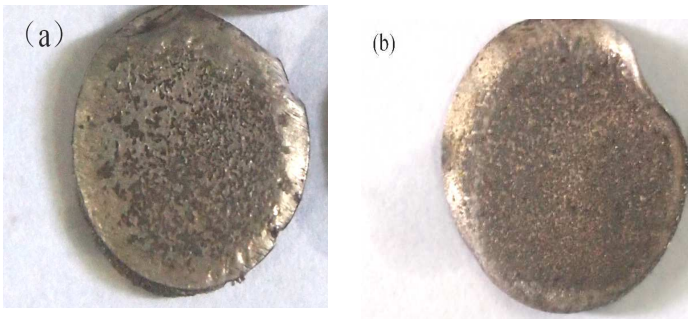

Fig. 11. Photos of the Li electrodes in cells with $LiNi_{0.5}Mn_{1.5}O_4$ synthesized by (a) ethanol-assisted hydrothermal method and (b) precipitation method after 400 cycles at 5 C rate.

The EIS measurements were performed on the cells before and after 200 cycles at 5 C rate. And the Nyquist plots are showed in Fig. 12. As shown, each plot consists of a depressed semicircle in the high frequency region and a sloping line at low frequency range. And the depressed semicircle reflects the interface impendence, including interfacial layer and charge transfer reaction.[30,31] It can be seen that the impendence of sample by ethanol-assisted hydrothermal method is smaller, before and after 200 cycles. The results indicate that the cell polarization of ethanol-assisted hydrothermal method is smaller during cycling, which is favorable to the cyclability.

The high temperature performances of $LiNi_{0.5}Mn_{1.5}O_4$ material were tested at 55 °C at a rate of 2 C and showed in Fig. 13. After 200 cycles, the discharge capacity of $LiNi_{0.5}Mn_{1.5}O_4$ by ethanol-assisted hydrothermal method is 101.4 mAh g^{-1} with capacity retention ratio of 82.0%, higher than 81.0% of precipitation method. The elevated temperature can accelerate the side reaction between $LiNi_{0.5}Mn_{1.5}O_4$ material and electrolyte. Although the sample of ethanol-assisted hydrothermal method has a larger specific active surface area, it still has a smaller capacity fading at elevated temperature. It benefits from its lower Mn^{3+} contents.[32~34] The Mn^{3+} ions tend to undergo a disproportionation reaction, leading to dissolution of Mn^{2+}. The dissolved Mn^{2+} migrates to the anode and deposits on the surface of anode, increasing anodic polarization. Besides the Jahn–Teller distortion causes the particle separation of $LiNi_{0.5}Mn_{1.5}O_4$.

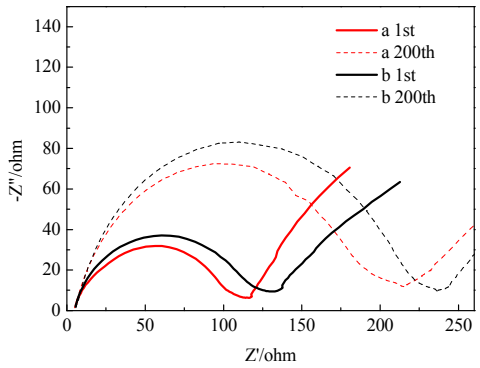

Fig. 12. Electrochemical impendence spectroscope curves of $LiNi_{0.5}Mn_{1.5}O_4$ synthesized by (a) ethanol-assisted hydrothermal method and (b) precipitation method before and after 200 cycles at 5C rate.

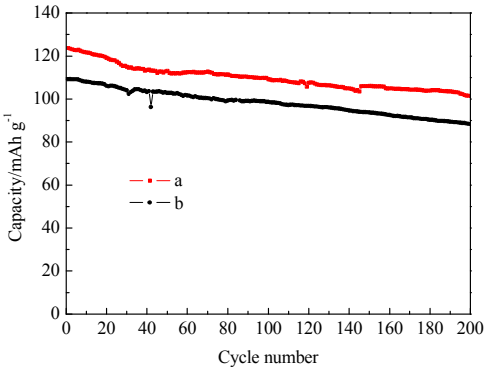

Fig. 13. Cycling performance of $LiNi_{0.5}Mn_{1.5}O_4$ synthesized by different methods at a rate of 2 C at 55 °C.

Conclusions

In this paper, the $LiNi_{0.5}Mn_{1.5}O_4$ material with excellent electrochemical performance was successfully synthesized by the ethanol-assisted hydrothermal method. The ethanol-assisted hydrothermal process decreases the size and aggregation degree of particles, leading to large specific active surface area and shorter Li^+ ions diffusion distance. On the other hand, the ethanol-assisted hydrothermal process improves the crystallinity and mixes the reagents homogeneously, leading to low impurity and Mn^{3+} ions contents. The low Mn^{3+} ions content can reduce dissolution of Mn^{2+} into the electrolyte resulted from the

Journal of Materials Chemistry A Accepted Manuscript

disproportionation reaction of Mn^{3+}, beneficial to cycle performance. The $LiNi_{0.5}Mn_{1.5}O_4$ material synthesized by ethanol-assisted hydrothermal method exhibits excellent rate capability with discharge capacities of 81.7 mAh g^{-1} at rate 20 C. What's more, after 1000 cycles at 5 C discharge rate, its discharge capacity is 102.1 mAh g^{-1} with capacity retention ratio of 88.1%. The excellent long-term cycling stability will promote the development of $LiNi_{0.5}Mn_{1.5}O_4$ material to meet practical application demands of LIBs.

Acknowledgements

We acknowledge the National Natural Science Foundation of China (Grant No. 21273058), China postdoctoral science foundation (Grant No.2012M520731), Heilongjiang postdoctoral financial assistance (LBH-Z12089) for their financial support.

Notes and references

[a] School of Chemical Engineering and Technology, Harbin Institute of Technology, No.92 West-Da Zhi Street, Harbin 150001, China
Tel: 86-451-86417853; E-mail: wangzhb@hit.edu.cn

1 J. Hassoun, K. S. Lee, Y. K. Sun and B. *J. Am. Chem. Soc.*, 2011, **133**, 3139.
2 J. H. Cho, J. H. Park, M. H. Lee, H. K. Song and S. Y. Lee, *Energy Environ. Sci.,* 2012, **5**, 7124.
3 J. B. Goodenough and K. S. Park, *J. Am. Chem. Soc.,* 2013, **135**, 1167.
4 J. Xiao, X. Chen, P. V. Sushko, M. L. Sushko, L. Kovarik, J.Feng, Z. Deng, J. Zheng, L. G. Gordon, Z. Nie, D. Choi, J. Liu, J. Zhang and M. S. Whittingham, *Adv. Mater.*, 2012, **24**, 2109.
5 X. Fang, M. Ge, J. Rong and C. Zhou, *J. Mater. Chem. A*, 2013, **1**, 4083.
6 X. Zhang, F. Cheng, J. Yang and J. Chen, *Nano letters*, 2013, **13,** 2822.
7 L. Zhou, D. Zhao and X. W. Lou, *Angew. Chem. Int. Ed.,* 2012, **124**, 243.
8 P. Strobel, A. I. Palos, M. Anne and F. L. Cras, *J. Mate. Chem.*, 2000, **10**, 429.
9 Y. J. Bai, C. Gong, N. Lun and Y. X. Qi, *J. Mater. Chem. A*, 2013, **1**, 89.
10 T. Ohzuku, A. Ueda and N. Yamamoto, *J. Electrochem. Soc.*, 1995, **142**, 1431.
11 X. Fang, M. Ge, J. Rong and C. Zhou, *J. Mater. Chem. A*, 2013, **1**, 4083.
12 Z. Chen, H. Zhu, S. Ji, V. Linkov, J. Zhang and W. Zhu, *J. Power Sources*, 2009, **189**, 507.
13 H. Wang, T. A. Tan, P. Yang, M. O. Lai and L. Lu, *J. Phys. Chem. C*, 2011, **115**, 6102.
14 X. Fang, N. Ding, X. Y. Feng, Y. Lu and C. H. Chen, *Electrochim. Acta*, 2009, **54**, 7471.
15 H. B. Kang, S. T. Myung, K. Amine, S. M. Lee and Y. K. Sun, *J. Power Sources*, 2010, **195**, 2023.
16 Y. Dong, Z. Wang, H. Qin and X. Sui, *RSC Adv.*, 2012, **2**, 11988.
17 Y. Sun, Y. Yang, X. Zhao and H. Shao, *Electrochim. Acta*, 2011, **56**, 5934.
18 R. Alcantara, M. Jaraba, P. Lavela and J. L. Tirado, *Electrochim. Acta*, 2002, **47**, 1829.
19 R. Santhanam and B. Rambabu, *J. Power Sources*, 2010, **195**, 5442.
20 J. Song, D. W. Shin, Y. Lu, C. D. Amos, A. Manthiramand and J. B. Goodenough, *Chem. Mater.,* 2012, **24**, 3101.
21 Q. Zhong, A. Bonakdarpour, M. Zhang, Y. Gao and J. R. Dahn, *J. Electrochem. Soc.* 1997, **144**, 205.
22 M.M. Thackeray, *J. Electrochem. Soc.* 1995,**142**, 2558.
23 Y. K. Sun, K. H. Lee, S. I. Moon and I. H. Oh, *Solid State Ionics*, 1998, **112**, 237.
24 J. H. Kim, S. T. Myung, C. S. Yoon, S. G. Kang and Y. K. Sun, *Chem. Mater.*, 2004, **16**, 906.
25 M. Kunduraci and G. G. Amatucci, *Electrochim. Acta*, 2008, **53**, 4193.
26 X. Zhang, F. Cheng, K. Zhang, Y. Liang, S. Yang, J. Liang and J. Chen, *RSC Adv.*, 2012, **2**, 5669.
27 N. Amdouni, K. Zaghib, F. Gendron, A. Mauger and C. M. Julien, *Ionics*, 2006, **12**, 117.
28 L. Si, L. Yue and D. Jin, *Cryst. Res. Technol.*, 2011, **46**, 1149.
29 H. I. Chen and H. Y C ang, *Coll. Surf. A*, 2004, **242**, 61.
30 L. J. Xi, H. E. Wang, Z. G. Lu, S. L. Yang, R. G. Ma, J. Q. Deng and C. Y. Chung, *J. Power Sources*, 2012, **198**, 251.
31 H. Fang, Z. Wang, , B. Zhang, , X. Li and G. Li, *Electrochem. Commun.*, 2007, **9**, 1077.
32 J. S. Park, K. C. Roh, J. W. Lee, K. Song, Y. I. Kim and Y. M. Kang, *J. Power Sources*, 2013, **230**, 138
33 B. J. Hwang, , Y. W. Wu, , M. Venkateswarlu, , M. Y. Cheng and R. Santhanam, *J. Power Sources*, 2009, **193**, 828.
34 B. Li, L. Xing, M. Xu, H. Lin and W. Li, *Electrochem. Commun.*, 2013, **34**, 48.

Journal of Materials Chemistry A Accepted Manuscript

Ethanol-assisted hydrothermal synthesis of $LiNi_{0.5}Mn_{1.5}O_4$ with excellent long-term cyclability at high rate for lithium-ion batteries

Contents entry

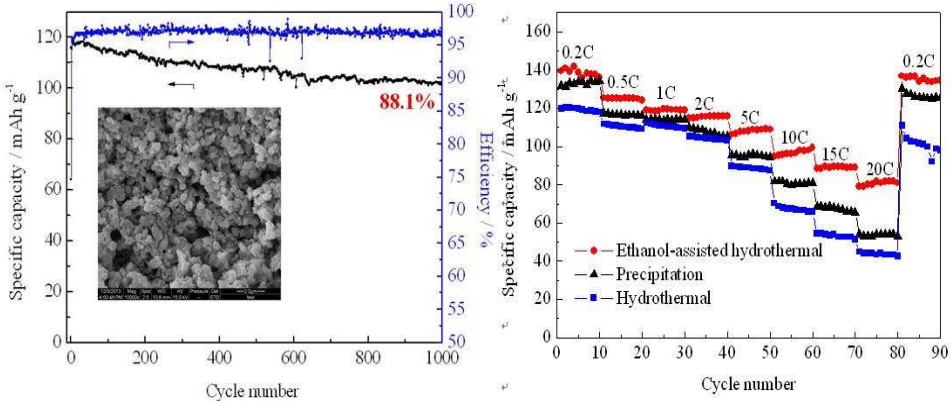

The $LiNi_{0.5}Mn_{1.5}O_4$ synthesized by ethanol-assisted hydrothermal method showed excellent rate performance and stable long-term cyclability.

Journal of Materials Chemistry A Accepted Manuscript